Lifetime of Charge Carriers in Multiwalled Nanotubes

M. Zamkov, N. Woody, B. Shan, Z. Chang, and P. Richard

James R. Macdonald Laboratory, Department of Physics, Kansas State University, Manhattan, Kansas 66506-2604, USA

(Received 6 October 2004; published 9 February 2005)

The nature of low-energy excitations in multiwalled nanotubes (MWNTs) is investigated by means of two-color time-resolved photoemission. A careful analysis of the ballistic transport, secondary excitations, and band structure effects was employed in order to extract single electron lifetimes from the observed relaxation trend. It is demonstrated that in the vicinity of the Fermi level the energy dependence of *e-e* scattering times is inversely proportional to approximately the square of the excitation energy. This result provides strong evidence that electron transport in MWNTs exhibits a Fermi-liquid behavior, indicating that long-range *e-e* interaction along the tube vanishes due to screening.

DOI: 10.1103/PhysRevLett.94.056803 PACS numbers: 73.21.–b, 73.22.–f, 73.23.–b, 79.60.Jv

Recently, carbon nanotubes have become a model system for the investigation of electronic transport in interacting one-dimensional quantum wires. The dominant role of Coulomb interactions in these systems may constrain electrons to form a Luttinger liquid (LL) [1,2], characterized by the purely plasmonic nature of low-energy excitations. Recent experiments [3,4] have provided sufficient evidence confirming the LL behavior in single walled nanotubes (SWNTs). Our understanding of electron transport in multiwalled nanotubes (MWNTs), on the other hand, still remains controversial [5–12], with observations ranging from ballistic transport, manifested, for instance, by the conductance quantization [8,9] to disordered multichannel wires [10–12].

One aspect of transport measurements in MWNTs is the difficulty of estimating the extent to which external sources, such as contacts in multijunction configurations, impurities, etc., influence the results. In addition, the presence of multiple conduction channels necessitates the individual treatment of each transmission mode. Therefore, an alternative experimental approach, not relying on the transport properties, would be useful in order to uncover the complex interplay of disorder and interactions in MWNTs.

As a viable alternative to transport measurements, we consider the temporal evolution of electronic excitations in the vicinity of Fermi level (E_F). According to recent *ab initio* calculations [13,14], dynamics of electron scattering in many real metals, where the phase space available for electronic transitions is large, can be successfully described within a Fermi-liquid theory (FLT). For these systems, one-electron excitations acquire finite lifetimes that are proportional to the square of the excitation energy, $(E - E_F)^{-2}$. This result, however, is not valid for one-dimensional structures, or LL, where the reduction of the number of independent momentum components freezes out all scattering processes so that the conventional electronic states are no longer well defined. The energy dependence of electron lifetimes in LL, therefore, is constrained to deviate from the FLT scaling, $\tau \propto (E - E_F)^{-2}$, which was experimentally confirmed for SWNTs in time-resolved photoemission (TRPE) measurements [15].

TRPE provides a unique and powerful tool for studying the relaxation dynamics of charge carriers on the ultrashort time scale. The extraction of a single electron lifetime from a TRPE signal, however, can be realized only if contributions from decay channels other than *e-e* scattering are negligible. Among the major pathways for the electron escape from the excited state are the ballistic transport away from the probed region and the generation of secondary electrons, often triggered by the relaxation of holes left in the valence band. Notably, for metallic probes where the conduction electrons are confined within the excitation volume, the energy dependence of relaxation times was found to be in excellent agreement with the $(E - E_F)^{-2}$ FLT scaling [16].

Here, we report on the energy dependence of the excited electron lifetimes in MWNTs, measured by means of time-resolved photoemission. A careful analysis of the MWNT band structure, ballistic drift, and the formation of the secondary Auger electrons has been performed. It is demonstrated that for sufficiently low energies of TRPE excitations, a valid comparison of measured lifetimes with FLT predictions becomes possible. The resulting relaxation trend is found to follow strictly the power-law energy dependence, $\tau \propto (E - E_F)^{-n}$ with $n \approx 2.07$. This result is consistent with Fermi-liquid behavior, indicating that the multidimensional nature of charge propagation should be invoked in modeling electronic properties of MWNTs.

The experiments were performed using the Kansas Light Source mode-locked Ti:sapphire laser system, generating 35 fs pulses at 790 nm. Frequency-tripled UV photons were produced through nonlinear effects during the photoionization of N_2 molecules. The resulting UV and IR beams were delayed with respect to each other and overlapped on the sample at a 30° incidence angle. Initially, the sample is perturbed by the IR pump beam with a photon energy of 1.57 eV, which promotes the electron population from below E_F into the conduction band. The resulting charge distribution, consisting of *e-h* pairs, is then probed

with a UV pulse that energetically exceeds the sample work function of 4.24 ± 0.05 eV by 0.47 eV [17]. In this configuration, energy dependent lifetimes of both the conduction electrons and the valence holes can be investigated [18]. To isolate the photoelectrons emitted from the excited states, we recorded the change in the photoemission induced by the IR pump pulse. The corresponding ''excitation'' difference reflects the nonequilibrium carrier distribution as induced by the pump pulse. Following the photoionization by the UV pulse, electrons drifted into the magnetically and electrically shielded 30-cm-long spectrometer tube and were detected with a backgammon position sensitive detector. The upper bound of the energy resolution in the present study was estimated to be 10 meV for 1 eV photoelectrons.

Samples of high-purity (>95%) individual MWNTs produced by the arc discharge method were used in the present study. As confirmed by STM measurements [19], the nanotube diameter range was 10–20 nm, which corresponds to about 20 to 30 coaxial SWNT shells. The experimental medium consisted of 0.4-mm-thick freestanding MWNT ''bucky'' paper, which was attached to a Ta substrate and outgassed in multiple heating and annealing cycles with a peak temperature of 700 K.

The average nanotube length was estimated to be 3–5 μm, which is considerably smaller than the laser spot size (beam diameter ≈ 400 μm). In this arrangement, the ballistic transport along the tube is not likely to remove a significant portion of excited electrons from the probed volume. The electron escape into the material is also strongly suppressed due to the extensive penetration of the UV probe photon (the optical skin depth ≈ 17 nm) through the MWNT wall. In the absence of any significant carrier migration from the probed region, the contribution from ballistic transport into experimental lifetimes can be neglected.

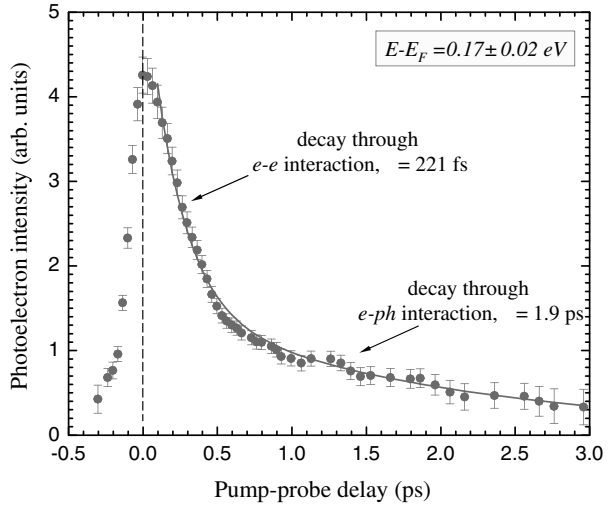

FIG. 1. The two-photon photoemission signal as a function of the pump-probe delay (cross-correlation trace) recorded for the conduction electrons at $E - E_F = 170 \pm 20$ meV. The experimental data are fitted with a biexponential curve utilizing the slow, $\tau_{e\text{-}e}$, and fast, $\tau_{e\text{-ph}}$, decay components (see text).

The temporal evolution of the photoexcited charge carriers was measured in the range of -0.4 to 3 ps. Figure 1 shows a typical cross-correlation trace recorded for an energy of $E - E_F = 0.17 \pm 0.05$ eV. The spectrum exhibits two different decay trends that were previously observed and characterized for the case of SWNT ropes [18]. The initial relaxation, represented by a fast decay component in Fig. 1, is attributed to the internal thermalization of the electronic system, which is primarily driven by *e-e* scattering processes. After the system returns to the Fermi-Dirac distribution it continues to decay with a slower rate associated with electron gas cooling by electron-phonon (*e*-ph) interactions. We evaluate the individual contributions for the two decay components, $\tau_{e\text{-}e}$ and $\tau_{e\text{-ph}}$, by fitting the experimental data with the convolution of the pump-probe correlation and a biexponential curve. Fortunately, the characteristic time scales for *e-e* and *e*-ph interactions are sufficiently different and thus easy to identify (see Fig. 1). Since the focus of the present study is *e-e* scattering processes, $\tau_{e\text{-ph}}$ is subtracted from the experimental cross-correlation signal and the remaining fast component, $\tau_{e\text{-}e}$, is investigated.

We shall now discuss the role of the MWNT band structure in the decay of electronic states. The relaxation of excited carriers is normally accompanied by the production of *e-h* pairs and, consequently, is subject to general constraints imposed by energy and momentum conservation. For some states that are characterized by a vanishing Fermi surface gradient, $\nabla_k E \rightarrow 0$, the decay would require a transfer of large momentum to the secondary excitations. As a result, the number of *e-h* pairs available for the corresponding energy and momentum change would be relatively small. In this case, electronic states are expected to acquire comparatively long lifetimes, which results in a local deviation from FLT-like power-law energy dependence. A vivid illustration of this concept is the observation of the anomalous energy dependence of electronic lifetimes in graphite, which was attributed to the presence of a saddle point in the π^* band at the M point [20].

Figure 2(a) shows the band structure for a (110, 110) SWNT ($d = 15$ nm), which represents a typical outer shell geometry in the investigated MWNT sample. The electronic structure is calculated in the vicinity of E_F by folding the graphite bands and utilizing the universal scaling for the density of states (DOS) [21]. We first concentrate on the decay of carriers from initial states, labeled as (1), where $\nabla_k E \rightarrow 0$. The corresponding spectrum for the secondary *e-h* pair excitations is displayed in Fig. 2(b). In order to illustrate the energy and momentum constraints on *e-e* scattering, we compare the *e-h* pair spectrum with the electron energy loss for a decay from the closest to E_F type 1 state [see Figs. 2(c) and 2(d)]. The dark shaded area

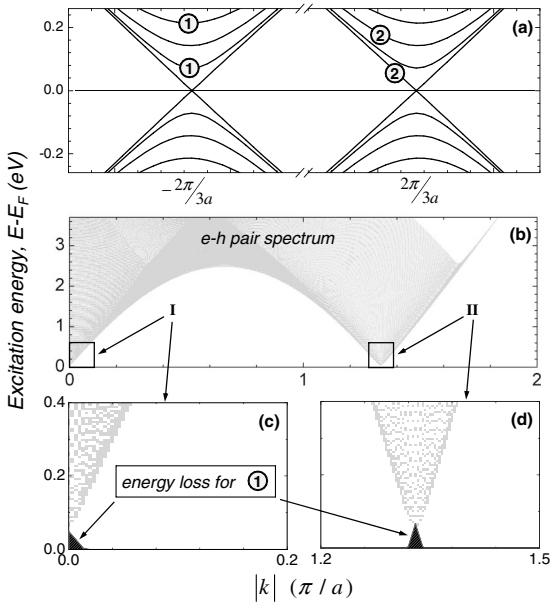

FIG. 2. (a) Energy bands in the vicinity of E_F, calculated for a (110, 110) SWNT. (b) Spectrum of e-h pair excitations, illustrating the energy-momentum constraints on electronic decay from the least energetic state labeled (1). (c),(d) The available phase space for an electron decay from the initial state labeled (1) is illustrated through the overlap of the e-h pair spectrum with energy-loss spectra.

represents all possible combinations of energy and momentum changes for an electron decay. The secondary excitations of e-h pairs, triggered by the decay, are then placed within the available phase space, displayed as the light shaded area. Since there is virtually no overlap between these two spectra, the phase-space volume available for the decay from the type 1 state through the excitation of e-h pairs is negligibly small, and the associated lifetimes will be elongated. In contrast, the electron decay from the initial state of type 2 is subject to the large available phase space, which ensures a valid comparison of the corresponding experimental lifetimes with FLT. Therefore, the correct determination of quasiparticle lifetimes from the TRPE signal is possible only for electronic excitations into states with energies not exceeding that of the lowest type 1 state [see Fig. 2(a)]. Evidently, the latter corresponds to the first Van Hove singularity (VHS) in a SWNT. As a result of averaging over all possible types of metallic shells within a MWNT, this VHS gives rise to the inhomogeneously broadened peak, shown in Fig. 3(c). Here we assume that all SWNT shells can contribute to the photoemission and that the abundance of different MWNT diameters in a sample obeys a Gaussian distribution. By probing the electron lifetimes in the energy interval confined between E_F and the VHS peak, we thus study the unsuppressed electron decay, for which a valid comparison of relaxation times with FLT predictions becomes possible.

The energy dependence of relaxation lifetimes, $\tau_{e\text{-}e}$, derived from the measured cross-correlation traces is shown in Fig. 3(a). We note that the experimental data represented by negative excitation energies, $E - E_F < 0$, reflect the temporal dynamics of valence holes. For positive excitations, $E - E_F > 0$, the observed energy dependence exhibits two different relaxation regimes. Close to the Fermi level, $0 < E - E_F \leq 70$ meV, the measured lifetimes follow the FLT-like power-law energy dependence [see Fig. 3(b)], whereas, for $E > 70$ meV, the best fit of experimental data, given by solid line in Fig. 3(a), indicates that τ is linear in the excitation energy. This result is in sharp contrast to the to power-law energy dependence, $\tau \sim (E - E_F)^{-n}$, dictated by FLT. The observed deviation, however, is simply the effect of band structure peculiarities discussed above. By comparing the energy threshold for the expected decay suppression, shown in Fig. 3(c) (broad peak), with the experimental relaxation trend, one can unambiguously attribute the breakdown of the power-law energy dependence to the presence of type 1 topologies in the MWNT bands. Notably, the resulting switchover en-

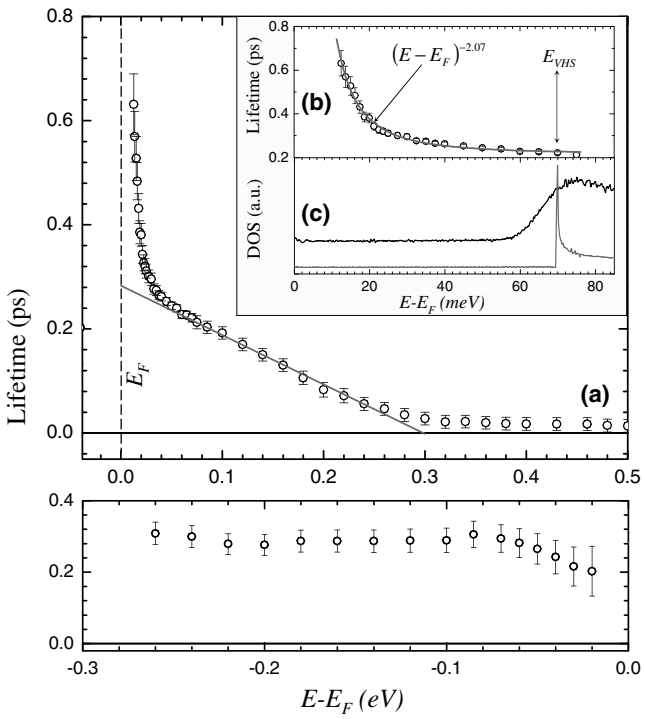

FIG. 3. Energy dependence of the excited electron lifetimes. (a) Close to E_F, the electron relaxation trend exhibits a FLT-like power-law energy dependence [see (b)]. However, for electron excitations that energetically exceed the first VHS, $E \geq E_{\mathrm{VHS}} \approx 70$ meV, the lifetime energy dependence is anomalous, $\tau \propto (E - E_F)^1$. Inset (b) ''zooms in'' on the energy interval, where the measured electron lifetimes are inversely proportional to approximately the square of the excitation energy. Estimated location of the first VHS in a (110, 110) SWNT (sharp peak near 70 meV), which, in the case a MWNT, containing a collection of different SWNT shells, becomes inhomogeneously broadened.

ergy ($70 < E < 80$ meV) is very near the estimated position of the first VHS ($E_{\mathrm{VHS}} = 70$ meV).

Generation of the secondary electrons can often lead to the deviation of the TRPE relaxation times from the lifetimes of the investigated electronic states. The dominant part of secondary excitations is triggered by the decay of laser created holes. Their relaxation is viewed as an Auger process, where one electron fills the hole and the released energy is transferred to the second electron, which is excited above E_F. Clearly, the production of the secondary electrons via an Auger decay is delayed from the initial direct photoexcitation by the lifetime of the hole. For example, the detailed analysis of the TRPE relaxation times on Cu [22] has shown that the secondary Auger excitations become dominant if the pulse duration exceeds the d-hole lifetime ($\tau_h \approx 35$ fs). On the contrary, when a shorter laser pulse is used ($\tau = 12$ fs), the contribution of Auger electrons is lowered to less than 10%. In the present work the average lifetime of photoinduced holes was measured to be 280 fs [see Fig. 3(a)], which defines the characteristic time scale for the delayed generation of the secondary Auger electrons. This time is long compared to the relaxation times of electronic excitations, and thus we conclude that the contribution of secondary electrons, although not negligible, is weak and not considered as potentially affecting the energy dependence of $\tau_{e\text{-}e}$.

Figure 3(b) ''zooms in'' on the energy interval, where the measured relaxation lifetimes are inversely proportional to the excitation energy. The solid curve represents the least square fit to the experimental data and is given by $\tau = (E - E_F)^{-2.07}$, where the absolute error in the determination of the exponent $n = -2.07$ is less than 0.1. The observed energy dependence is in excellent agreement with predictions within the Fermi-liquid paradigm for multidimensional systems. Based on this result, we speculate that the long-range e-e interaction in MWNTs is screened effectively by the excitation of plasmons in the surrounding electron system. This screening determines the character of low-energy excitations, which appears to be individual (one electron) rather than collective.

In conclusion, we have studied the temporal evolution of electronic states in MWNTs, by means of a femtosecond time-resolved photoemission. A careful analysis of the ballistic transport, secondary excitations, and band structure effects was performed in order to extract single electron lifetimes from the observed relaxation trend. It is demonstrated that in the vicinity of the Fermi level the energy dependence of e-e scattering times is inversely proportional to approximately the square of the excitation energy. This result is in excellent agreement with Fermi-liquid paradigm, indicating that long-range e-e interaction in MWNTs vanishes due to screening. The associated character of the charge propagation in MWNTs agrees well with two- or three-dimensional transport.

This work was supported by the Chemical Sciences, Geosciences, and Biosciences Division, Office of Basic Energy Sciences, Office of Science, U.S. Department of Energy.

[1] M. Bockrath *et al.*, Nature (London) **397**, 598 (1999).
[2] Z. Yao, H. W. Ch. Postma, L. Balents, and C. Dekker, Nature (London) **402**, 273 (1999).
[3] H. W. Ch. Postma, T. Teepen, Z. Yao, M. Grifoni, and C. Dekker, Science **293**, 76 (2001).
[4] B. Gao, A. Komnik, R. Egger, D. C. Glattli, and A. Bachtold, Phys. Rev. Lett. **92**, 216804 (1998).
[5] A. Bachtold *et al.*, Phys. Rev. Lett. **87**, 166801 (2001).
[6] E. Graugnard *et al.*, Phys. Rev. B **64**, 125407 (2001).
[7] W. Yi, L. Lu, H. Hu, Z. W. Pan, and S. S. Xie, Phys. Rev. Lett. **91**, 076801 (2003).
[8] S. Frank *et al.*, Science **280**, 1744 (1998).
[9] A. Urbina, I. Echeverria, A. Perez-Garrido, A. Diaz-Sanchez, and J. Abellan, Phys. Rev. Lett. **90**, 106603 (2003).
[10] R. Egger and A. O. Gogolin, Phys. Rev. Lett. **87**, 066401 (2001).
[11] E. G. Mishchenko, A. V. Andreev, and L. I. Glazman, Phys. Rev. Lett. **87**, 246801 (2001).
[12] A. Kanda, K. Tsukagoshi, Y. Aoyagi, and Y. Ootuka, Phys. Rev. Lett. **92**, 036801 (2004).
[13] F. Ladstädter *et al.*, Phys. Rev. B **68**, 085107 (2003).
[14] I. Campillo *et al.*, Phys. Rev. B **61**, 13 484 (2000).
[15] T. Hertel and G. Moos, Chem. Phys. Lett. **320**, 359 (2000).
[16] J. Cao, Y. Gao, H. E. Elsayed-Ali, R. J. D. Miller, and D. A. Mantell, Phys. Rev. B **58**, 10 948 (1998).
[17] M. Zamkov *et al.*, Phys. Rev. Lett. **93**, 156803 (2004).
[18] T. Hertel, R. Fasel, and G. Moos, Appl. Phys. A **75**, 449 (2002).
[19] NanoLab, Inc., 55 Chapel Street Newton, MA 02458, USA.
[20] G. Moos, C. Gahl, R. Fasel, M. Wolf, and T. Hertel, Phys. Rev. Lett. **87**, 267402 (2001).
[21] J. W. Mintmire and C. T. White, Phys. Rev. Lett. **81**, 2506 (1998).
[22] R. Knorren, G. Bouzerar, and K. H. Bennemann, Phys. Rev. B **63**, 094306 (1998).